ELSEVIER
Advances in Water Resources 23 (1999) 177–187
Advances in Water Resources

A geomorphology-based semi-distributed watershed model

Jozsef Szilagyi [a,*], Marc B. Parlange [b]

[a] Conservation and Survey Division, University of Nebraska-Lincoln, 113 Nebraska Hall, Lincoln NE 68588-0571, USA
[b] Department of Geography and Environmental Engineering, The Johns Hopkins University, Baltimore MD 21218-2686, USA

Received 12 April 1998; received in revised form 28 October 1998; accepted 6 April 1999

Abstract

A semi-distributed watershed model was developed that conceptualizes the catchment as a cascade of nonlinear storage elements whose geometric dimensions are derived from the Horton–Strahler ordering of the stream network. Each storage element represents quick storm runoff over land or in a channel segment. The physically based groundwater submodel is parameterized through the application of the Brutsaert–Nieber recession flow analysis and it provides continuous baseflow separation. The model requires the calibration of seven parameters from a one year rainfall–runoff record. It was tested on the Mahantango Creek watershed in the Susquehanna River basin, Pennsylvania. © 1999 Elsevier Science Ltd. All rights reserved.

1. Introduction

Much hydrologic research has focused on the identification of linkages between the geomorphology of a catchment and its hydrologic response [11]. One approach has been the use of statistical methods, mostly regression techniques, to identify the linkages between geomorphology and runoff for a particular catchment [34]. A second approach has been to identify physical parameters of the watershed in transporting rainfall excess through the catchment like the geomorphological unit hydrograph (GUH) theory [25]. The GUH concept makes use of Horton's laws [15] of network parameters. The GUH is the probability density function of runoff arrival times at the outlet of the catchment resulting from rain of a unit depth uniformly distributed over the watershed. The water is routed through the stream network of the catchment with Markovian transition probabilities between channel segments of different Horton–Strahler [27] stream orders. The transition probabilities are related back to network characteristics (e.g. the Horton ratios of stream numbers, stream lengths, and associated subcatchment areas) to obtain the GUH. The GUH concept is based on the assumption of a linear catchment response to precipitation and does not explicitly consider subsurface processes.

Another geomorphologic approach to watershed modeling is TOPMODEL, introduced by Beven and Kirkby [6]. While the GUH concept places an emphasis on the drainage network of the catchment in the hydrologic response of the watershed, TOPMODEL focuses on the role of topography in runoff generation [20]. TOPMODEL simulates the dynamics of runoff contributing areas using a spatially varying topographic index. TOPMODEL appears to give reasonable runoff estimates in comparison with measured streamflow for hilly terrain with thin soils [7]. A basic problem with the application of the topographic index is that the actual form of its distribution function depends on the grid size of the digital elevation model leading to grid size dependent model parameter values that may have no physical interpretation at large grid sizes [5].

In this paper we present a watershed model which has an overall structure known as the geomorphologic nonlinear cascade (GNC) [3]. The GNC is a mix between the GUH concept and the reservoir cascade theory which in the linear case is the Nash [19] cascade. The GNC approach treats the quick storm runoff mechanisms from the watershed as a cascade of partially parallel nonlinear reservoirs. The runoff paths are derived from the Horton–Strahler ordering scheme of the catchment stream network. In Fig. 1(a) a sample Horton–Strahler ordered stream network is presented where the corresponding subcatchments and channel sections are delineated. The subcatchments have the

* Corresponding author. Tel.: 001-402-472-3471; fax: 001-402-472-2410; e-mail: szilagy@unlinfo.unl.edu

0309-1708/99/$ - see front matter
PII: S0309-1708(99)00021-4

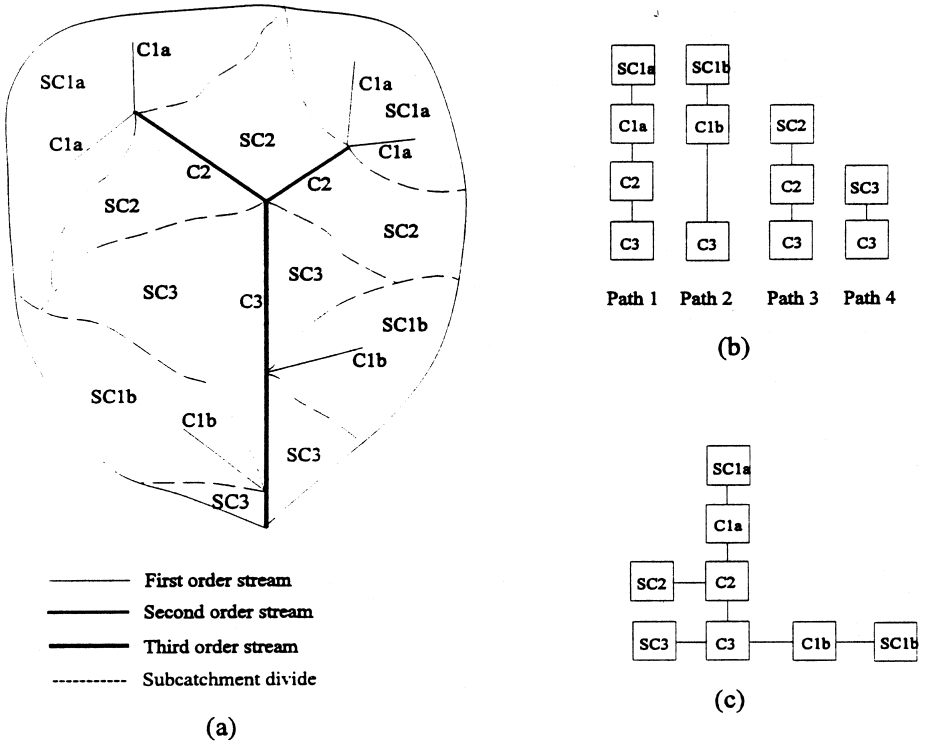

Fig. 1. (a) Horton–Strahler ordered sample stream network (SC: subcatchment, C: channel section). (b) Corresponding cascades of storage elements according to the possible paths a drop of rain may travel within the quick storm response of the catchment. (c) Spatial connectivity of the storage elements.

same ordering number as the stream section located within the subcatchment. In Fig. 1(b) each pathway represents a subcatchment of varying order and a collection of channel sections within the watershed. In Fig. 1 the first order storage elements are further divided into subgroups 'a' and 'b' according to the stream pathway they feed into. The different travel paths can only be treated independently if the storage element outflows are linear. Since the storage outflows in the model are assumed to be nonlinear, their spatial connectivity is important (see Fig. 1(c)).

Since the GNC model of Berod et al. [3] accounted for only quick storm response, we extend the model to include evaporation, soil moisture, groundwater recharge, and baseflow to the stream. Inclusion of baseflow is important because during extended periods of no precipitation the flow in the stream network is often entirely generated by groundwater and also in catchments with flat topography and shallow rooted vegetation baseflow contribution to total streamflow may become dominant on an annual basis.

It should be noted that the information content of rainfall–runoff records justifies the calibration of perhaps only half a dozen parameters in a watershed model [16]. As a consequence, it is important to define independent of the rainfall–runoff record as many of the physical parameters as possible. This is done through the combination of hydrologic analysis of streamflow records [28,29] and Geographic Information System (GIS) analysis of the watershed.

This model represents efforts to: (a) retain the nonlinear nature of watershed response to precipitation; (b) minimize the number of parameters to be optimized based on the discharge record while retaining the most important physical processes involved; and (c) estimate as many model parameters as possible from the geomorphological characteristics of the watershed.

2. Model description

The building block of the model is a general nonlinear storage–discharge relationship for the hydrologic cascade elements depicting surface and quick subsurface runoff:

$$Q = kV^n, \tag{1}$$

where k is the storage parameter [$m^{3(1-n)}$ s^{-1}] and n [–] an exponent. If n is unity the storage reservoir is linear and k is the inverse of the average residence time. The catchment is described by a set of partly parallel cascades that represents the family of all possible paths that a raindrop may follow when traveling from its landing point to the outlet (see Fig. 1). The order of the elements in the possible paths are the following [3]: the first element is always an overland region, the last one is the

outlet, and in between are the channel elements. The model assumption that each raindrop lands on the surface of a subcatchment is supported by the observation that in most catchments more than 95% of the catchment area is occupied by land surface [3]. Each element of the cascade is represented by a nonlinear reservoir in regard to quick storm response, infiltration or channel routing. The storage element is represented as a rectangular slab [3] for which the stored water volume can be formulated as

$$V = fwLh, \tag{2}$$

where f is the effective porosity or specific yield [–], w and L are the width and length of the slab respectively, and h the water table depth. For storage elements representing quick storm and channel response f is taken to be unity. L is the mean length of the channel sections of specified order and path and w is AL^{-1} for subcatchments, where A is the mean area of the subcatchments of specified order and path.

For quick storm response both in the channel and in the subcatchment we use the kinematic wave approach [18]

$$Q = \alpha w h^m, \tag{3}$$

where α is a parameter [m^{2-m} s^{-1}] that combines the slope and friction coefficients and m a constant exponent which is optimized from the rainfall–runoff records. Combining Eqs. (1)–(3) and equating n and m,

$$k = \alpha f^{-n} w^{1-n} L^{-n}. \tag{4}$$

In order to keep the number of parameters to be optimized to a minimum the same constant, α_{sc}, is assigned to each storage element representing subcatchments and another constant, α_c, to each storage element that represents channel sections. The value of n is fixed for all of the storage elements (regardless of subcatchment or channel). Hence there are 3 unknown parameters (α_{sc}, α_c, n) which need to be optimized. The inputs to quick storm runoff are calculated in the infiltration submodel after accounting for interception losses.

A schematic of the basic physical processes modeled within a subcatchment is displayed in Fig. 2.

The interception was calculated using an exponential loss function and a very simple method of accounting for the antecedent precipitation status.

The infiltration was calculated using the Holtan model [13]. The initial potential water storage space was estimated using tabulated rooting depth values [30] for the different land cover and soil texture combinations derived from digitized USGS land use, land cover and USDA soil maps.

The potential evaporation values [17] were further modified [4] according to the stored water in the root zone when estimating actual evaporation.

Deep percolation in the model is allowed at a constant rate [13] whenever the soil moisture storage exceeds field capacity. Water – other than quick subsurface flow, which is incorporated in the quick storm runoff component – in the unsaturated zone is allowed to move only vertically in the model.

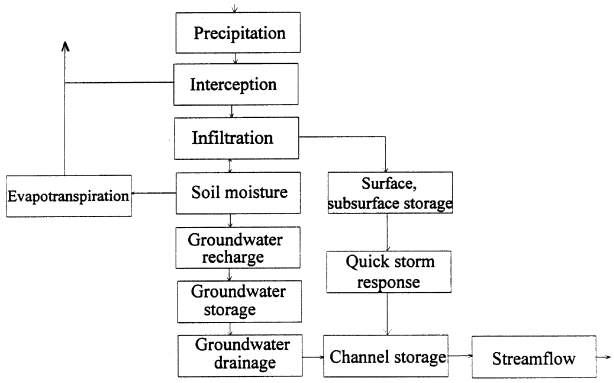

Fig. 2. Schematic diagram of the hydrologic components accounted for in the model.

Changes in the saturated zone are modeled again by a nonlinear storage reservoir. The concept is justifiable on the basis that the analytical solutions of unconfined groundwater drainage display a behavior characteristic of a single storage element with varying degree of nonlinearity [10] depending on the geometry of the system.

The equations applied in the submodels are presented in Appendix A.

3. Model application

3.1. Study area description

The model was tested on the Mahantango Creek watershed in east-central Pennsylvania. The watershed is a tributary of the Susquehanna River which is located in the non-glaciated part of the North Appalachian Ridge and Valley Region with a mean elevation of 200 m (the elevation range is 130–450 m).

The geology of the Mahantango watershed can be described, going from northwest to southeast, as folded Pennsylvanian sandstone and shale, Mississippian sandstone and shale, and Devonian sandstone, siltstone, and shale [22,32]. The moderately weathered channery or stony loam soils, characteristic of the catchment, are thin (1–3 m) with poorly developed horizons [1]. Land use is predominantly woodland (more than 70% of the catchment area) consisting of mixed hardwoods of oak, hickory, and poplar. The catchment area is 423 km^2 [2] and the total length of the perennial streams is 287 km. The main channel is 27 km in length. The hourly precipitation and daily runoff data used in our study cover a 6-year period between 1989 and 1995. The gauging station is situated near Dalmatia, the precipitation station is at Klingerstown close to the central part of the

watershed, and the mean monthly temperatures were recorded at Harrisburg, some 20 km distance from the watershed.

The topography of the catchment was derived from the US Geological Survey's 30-metre resolution Digital Elevation Model (DEM), resampled to 25 m to allow for proper overlays with other data covers [22]. The stream network of the watershed is based on the 1–100,000 scale USGS Digital Line Graph coverage. Fig. 3 presents the Horton–Strahler ordering of the streams in the watershed, and the corresponding subcatchments are displayed in Fig. 4. Fig. 5 depicts all the possible runoff paths and their spatial connectivity for a fourth order catchment. The area of the storage elements with the corresponding channel lengths for the watershed is listed in Table 1.

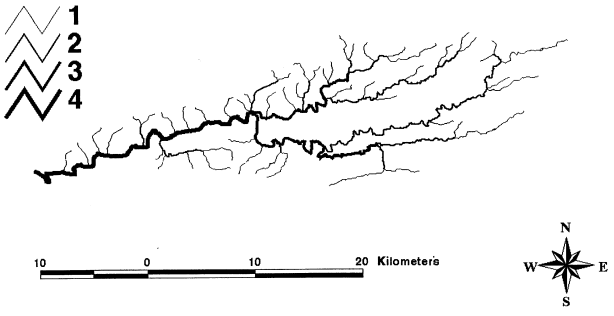

Fig. 3. Horton–Strahler ordered stream networks, Mahantango Creek, PA.

The physical soil texture categories of the watershed were derived from the Soil Service Geographic Data Base (SSURGO) which in turn was digitized from orthophotographs using county level soil survey reports [22]. The land use and land cover classes were derived from low-altitude infrared aerial photographs, Landsat TM and AVHRR imagery that were eventually converted into a GIS coverage [22]. Combining land use–land cover and soil type data an average estimated root depth (RD) value for each storage element of the watershed could be assigned by weighting the root depth values of the different land use–land cover and soil texture combinations [24,30] with the relative area of the given combination within each subgroup. Estimates of drainable porosity, field capacity and saturated hydraulic conductivity for the different storage elements can be obtained similarly to the rooting depth, except that they are a function of soil texture only. Table 2 displays the catchment representative physical soil parameters.

3.2. Model calibration

To parameterize the groundwater submodel we plotted (on a double-logarithmic graph) the observed daily mean runoff values against the rate of change in runoff between consecutive days (see Fig. 6) at least 5 days after any rainfall had been observed [28]. Following Brutsaert and Nieber [10] the lowest envelope of the data points represents the pure baseflow recession rate. In Fig. 6 a line with slope (b) of 1.5 was drawn.

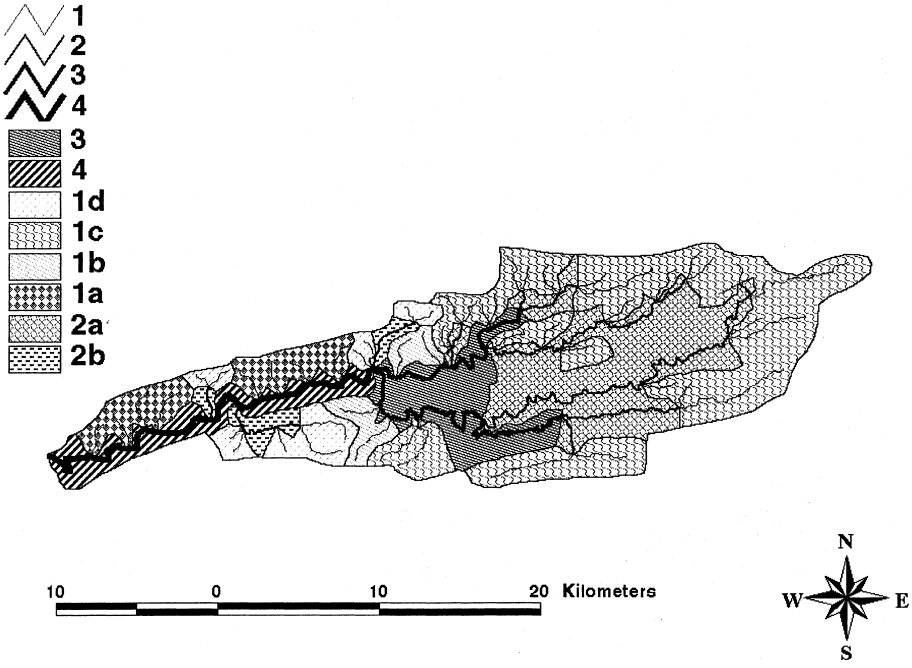

Fig. 4. Horton–Strahler ordered stream networks with the corresponding subcatchments marked according to possible pathways, Mahantango Creek, PA.

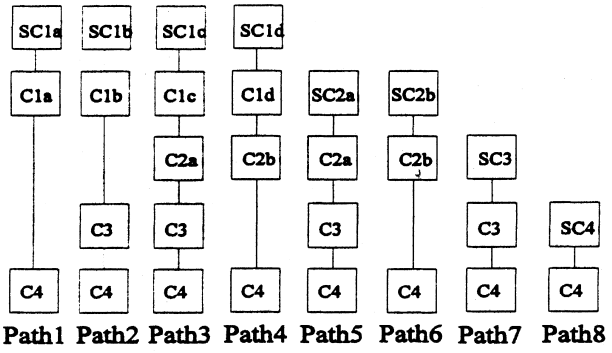

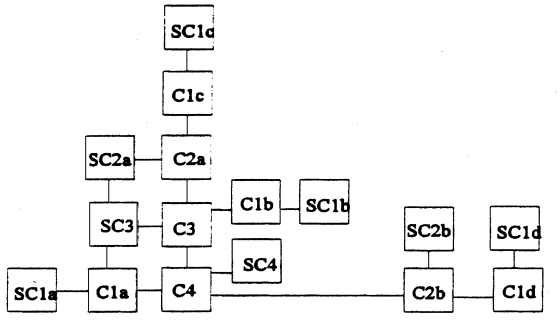

Fig. 5. Possible runoff paths and spatial connectivity of the storage elements for a fourth order catchment.

Table 1
DEM extracted channel lengths and subcatchment areas according to stream order and runoff path, Mahantango Creek, PA

Strahler order	Runoff path	Channel length (km)	Subcatchment area (km^2)
Fourth		27	34
Third		36	47
Second	a/	67	101
	b/	13	13
First	a/	21	32
	b/	13	16
	c/	89	152
	d/	21	28
Total		287	423

98% of the data points lie above this lower envelope line. An interception value, $a = 2.07 \times 10^{-7}$, results where the lower envelope crosses the unit discharge value. From Eq. (A.12) the unknown parameters n_{gw} and k_{gw} of the groundwater submodel are obtained as 2 and 1.07×10^{-14} m^{-3} s^{-1} for the watershed.

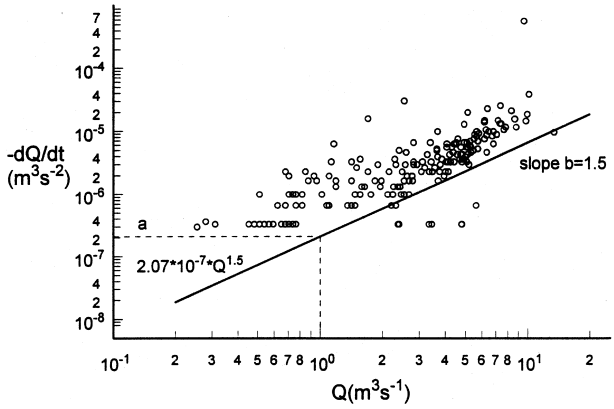

Fig. 6. Change in mean daily discharge rates vs mean daily discharge rates. The data displayed were taken at least 5 days following precipitation, the lines are the 98% lower envelopes, Mahantango Creek, PA, 1984–1987.

In the evaporation calculations (A.8), values of 0.188 and 0.539 (for the N 41° latitude) were assigned, for the constants d and e, respectively [2]. There are altogether seven parameters, three (α_{sc}, α_c, n) in the general nonlinear storage equations, two (β, γ) in the interception, and another two (k_i, n_i) in the infiltration submodels, which must be optimized. The following objective function was designed for the optimization of the last four parameters:

$$F = \sum_i (Q - Q'_{bf})^2 + g \sum_j (Q - Q'_{bf})^2, \quad (5)$$

where Q is the observed mean daily runoff, Q'_{bf} the simulated baseflow, g an arbitrary weight, j designates days with no precipitation and at least 5 days apart from the last day with reported precipitation, and i marks any other days. Typically g is chosen to be on the order of 10^3 when $Q'_{bf} > Q$ on a drought period day, and is unity otherwise. This formulation of the objective function assures that during assumed drought flow periods the optimized baseflow remains close to the observed runoff. The application of Eq. (5) enables us to separate the baseflow process from the quick storm response of the catchment and at the same time provides us with the hourly amounts of water (through the optimized infiltration parameters k_i and n_i) that are input to the quick storm response submodel. The remaining three parameters (α_{sc}, α_c, and n) are optimized within the quick storm response submodel by minimizing the mean square error term between simulated and observed runoff values.

Table 2
GIS derived catchment representative values of the physical soil parameters

Watershed	Effective porosity (%)	Field capacity (%)	Saturated hydraulic conductivity (10^{-6} m s^{-1})	Rooting depth (m)
Mahantango	45.0	28.4	1.8	1.5

The optimization was carried out by systematically incrementing the values of the parameters within a predefined range for each parameter.

Before proceeding with the application of Eq. (5) several considerations had to be made. Since watershed-scale soil moisture measurements are generally not available, an optimization period had to be chosen for which the change in soil moisture status (ΔSM) could be neglected (i.e. $\Delta SM \approx 0$). A period of about one year was obtained starting and ending in the fall when the catchment reaches the driest state between years. Since the initial soil moisture condition is not known, it also had to be optimized. During the optimization it had to be ensured that by the end of the period the simulated soil moisture would be close to its initial value. This is necessary to meet the prescribed $\Delta SM \approx 0$ condition. Starting the simulations in the driest period ensures that the observed runoff is mainly baseflow, thus the initial value of the baseflow process is known. We note here that normally snow accumulation is not of major importance in the Susquehanna River basin [22], that is why the model does not have a snow component. Table 3 displays the resulting optimized parameter values within their predefined intervals.

4. Results

The calibration period we chose for the Mahantango Creek watershed was November 1991–October 1992. The baseflow and total runoff for the calibration period are shown in Fig. 7 together with the measured mean daily runoff and daily precipitation sums. The highest simulated and observed runoff values are found in spring when the unconfined aquifer becomes recharged and loses water later through the rest of the year. It is the most pronounced in Fig. 8 where the time series of simulated and measured outflow are presented for an 11-month verification period (November 1992–September 1993). In Fig. 9 the simulated and measured cumulative values of the different hydrological processes during the verification period for the watershed are presented. It is interesting to observe from the graph how the interception and evaporation become important with the onset of the spring season. By the end of the period (September) the loss of water vapor to the atmosphere accounts for about half (55%) of the total precipitation. Fig. 10 is a plot of all simulated versus measured daily mean runoff values ($R^2 = 0.67$) for Mahantango Creek. Note that the best fit curve is almost on top of the unit slope line indicating only a slight model undershoot in the mean daily runoff values. Table 4 summarizes the model performance. The correlation coefficients between simulated and observed mean daily and monthly discharges are over 0.8 in most years.

Table 5 displays the water balance components over the catchment. Runoff is about half of the precipitation the watershed receives, while interception losses amount to one quarter of it. When evaporation and interception losses are combined they sum up to 55% of the total precipitation. Baseflow is 22% of the observed runoff. The relatively low level of baseflow contribution to total runoff can probably be explained by the varied topography of the watershed. Also, thin soils in the catchment allow trees to tap on the groundwater for meeting their transpiration needs as is often observed in forested mountainous watersheds [12].

So far we have dealt only with spatially aggregated outputs of the model, since usually these aggregates, like the runoff at the outlet, can easily be matched with measured data. However, the majority of the model outputs are spatially distributed over the subcatchments of the modeled watershed. Fig. 11 displays the spatial distribution of the simulated soil moisture (as percentage of the field capacity) content of the Mahantango catchment at the end (25 November 1992) of the

Table 3
Optimized parameter values and their optimization intervals, Mahantango Creek, PA

Submodels	Optimized parameter values	Optimization intervals
Interception submodel		
β (winter)	0.1	(0–1)
β (summer)	0.9	(0–1)
γ (winter)	0.1	(0–1)
γ (summer)	0.9	(0–1)
Evapotranspiration submodel		
BS/DL	0	(0–0.8)
Infiltration submodel		
k_i ($m^{-0.9}$ s^{-1})	8.780×10^{-9}	(10^{-12}–10^{-3})
n_i	1.3	(0.1–3)
SM_{init}	$0.7 \times FC$	(0.2FC–FC)
Quick storm response submodel		
n	2.0	(0.1–3)
α_{sc} (s^{-1})	0.555	(0.001–10)
α_c (s^{-1})	0.277	(0.001–10)

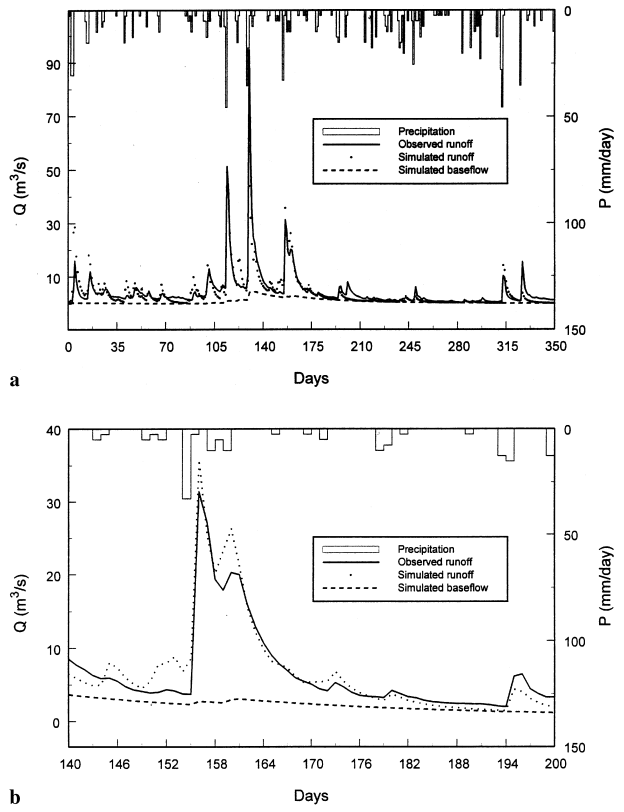

Fig. 7. Observed daily mean runoff and precipitation, simulated daily mean runoff and baseflow, Mahantango Creek, PA. (a) Calibration period: November 1991–October 1992. (b) Selected flood events within the calibration period.

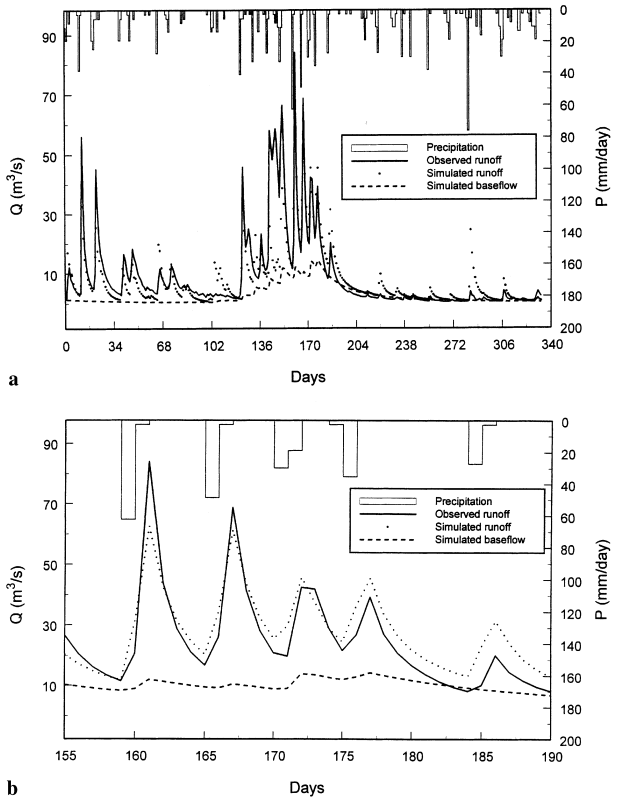

Fig. 8. Observed daily mean runoff and daily precipitation, simulated daily mean runoff and baseflow, Mahantango Creek, PA. (a) Verification period: November 1992–September 1993. (b) Selected flood events within the verification period.

optimization period. Similar maps can be constructed for any hour of any day for the following hydrologic characteristics of the catchment: infiltrated water volume, recharge to groundwater, available water volume for quick storm response, and channel storage. In general, with the growing size of the watershed modeled the spatial distribution of these hydrologic characteristics may become more important. In this respect, improved information on precipitation distribution (e.g. Radar derived) would be most valuable for future modeling efforts.

As a final assessment of the model, a simple sensitivity analysis of the optimized parameters is carried out for the Mahantango watershed by systematically changing the value of the selected model parameter and tracking the model's response in terms of mean squared errors between simulated and observed daily mean runoff. Fig. 12 (a) and (b) displays the result of the sensitivity test. The model is most sensitive to changes in the exponent of the infiltration equation (A.4) (i.e. it expresses the steepest slopes). This is not surprising since infiltrated water is distributed as recharge to soil moisture, and eventually groundwater and quick storm response. Once the amount of water available for quick storm response is determined, the parameters (α_{sc}, α_c and n) in the quick storm response submodel govern only the routing of this water volume through the catchment. The second most sensitive parameter is the initial soil moisture content value which we had to estimate due to the lack of measured data. Interestingly,

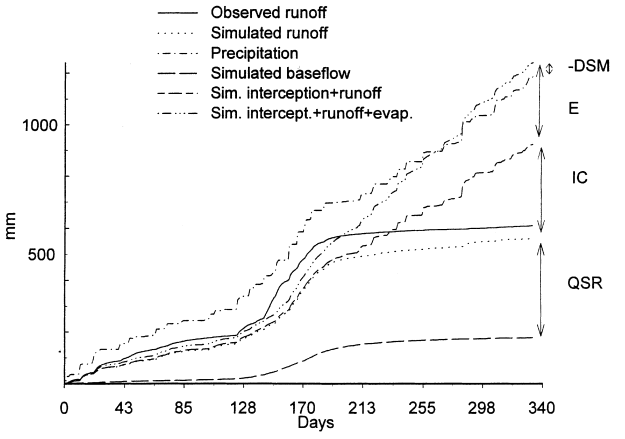

Fig. 9. Cumulative baseflow, quick storm response, QSR (= simulated runoff − baseflow), interception (IC), evaporation (E), and precipitation values, Mahantango Creek, PA. Verification period: November 1992–September 1993. DSM is the change in soil moisture status between the end and start of the period.

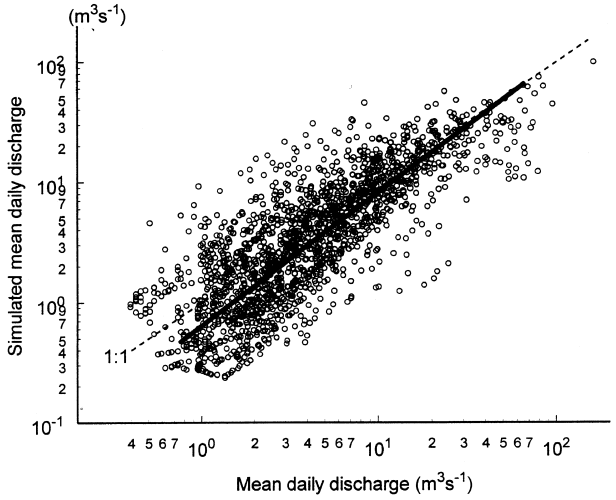

Fig. 10. Simulated versus observed mean daily runoff values, Mahantango Creek, PA. September 1989–September 1990; November 1991–August 1995. Solid line is the best fit curve, intermittent line represents the unit slope.

there is a relatively wide range of this value to which the model is not too sensitive (between 0.5 and 1 times the optimized value that was $0.7 \times FC$).

5. Summary

A nonlinear, semi-distributed model for simulating watershed dynamics is introduced. The model utilizes spatially distributed physical characteristics of the catchment with a minimum number (7) of parameters to be calibrated from rainfall–runoff records. The geomorphologic nonlinear cascade description for the quick storm response is based on the Horton–Strahler ordering of the stream network. The model was tested on the Mahantango Creek watershed within the Susquehanna River basin in Pennsylvania. Its performance for the catchment suggests the viability of building a nonlinear, semi-distributed, parameter-parsimonious watershed model that is able to simulate the most important hydrological processes in the catchment: interception, evapotranspiration, infiltration, quick storm response, recharge to groundwater and baseflow.

Acknowledgements

Partial support from the EPA grant on climate change and human health is gratefully acknowledged by the authors.

Appendix A

A.1. The interception submodel

Interception is that portion of precipitation that does not contribute to the soil moisture, groundwater or streamflow of the drainage basin [26]. Most of the intercepted water is retained in the vegetation cover of the catchment while a much smaller part is retained on rocks, buildings, etc. and eventually all is evaporated back to the atmosphere. The percentage of intercepted water can be substantial, for instance it may exceed one-third of the annual precipitation for coniferous forests [31]. A good physical description of the interception process does not exist at present. The exponential loss function is employed in our model to account for the interception loss [14,33] IC [m s^{-1}]

$$\mathrm{IC} = P e^{A+B(t'-1)} = P\beta\gamma^{(t'-1)}, \tag{A.1}$$

where P is the observed precipitation rate [m s^{-1}], β and γ are unknown parameters [–] which must be optimized and t' a time-index which is set to unity if there was no precipitation in the previous 24-hour period and is incremented by one with every new time step (1 h) after precipitation was recorded. Two independent sets of the parameters (β, γ) are employed, one for winter and one for summer.

A.2. The infiltration submodel

The volume of infiltrated water is calculated based on the Holtan [13] model which is able to account for both saturation and infiltration excess runoff production

Table 4
Summary statistics on model performance

Mahantango Creek, PA	Correlation (r) between daily values		Correlation (r) between monthly values	
	r (Q_s, Q_o)	$r(P, Q_o)$	$r(Q_s, Q_o)$	$r(P, Q_o)$
1991–1992 [a]	0.87	0.18	0.91	0.40
1992–1993	0.83	0.07	0.93	0.67
1993–1994	0.75	0.23	0.90	0.37
1994–1995	0.77	0.19	0.81	0.72
1989–1990	0.80	0.14	0.89	0.43

[a] Optimization period.
P: daily/monthly sum of precipitation; Q_o: mean daily/monthly runoff; Q_s: model simulated mean daily/monthly runoff.

Table 5
Catchment water balance components

	Mahantango Creek, PA
Number of periods considered	5
Precipitation [a] (P, mm/period)	1100
Runoff [a] (R, mm/period)	532
Baseflow (B, mm/period)	116
Interception (IC, mm/period)	289
Evaporation (E, mm/period)	323
R/P (%)	48
E/P (%)	29
IC/P (%)	26
$(E + \mathrm{IC})/P$ (%)	55
B/P (%)	11
B/R (%)	22

[a] Measured values.

mechanisms. The infiltration rate i [m s^{-1}] is given by means of a general storage equation where the actual storage is replaced by V_i, the potential storage space [m^3]

$$i = \frac{k_i V_i^{n_i}}{A} + l_s, \tag{A.2}$$

where l_s [m s^{-1}] represents a steady seepage rate toward the saturated zone when the stored water volume is greater than the soil's maximum available storage space (V_{i0}) times the field capacity (FC), otherwise it is taken to be zero. k_i [$m^{3(1-n_i)}$ s^{-1}] and n_i [–] are the storage parameter and exponent of the soil. The lumped continuity equation for the soil is

$$\frac{dV_i}{dt} = A(l_s - i). \tag{A.3}$$

Substituting Eq. (A.2) into Eq. (A.3) we obtain

$$\frac{dV_i}{dt} = -k_i V_i^{n_i} \tag{A.4}$$

which is the equation for the potential storage space calculations. Coupling Eq. (A.4) with Eq. (A.2) the time varying infiltration rate can be estimated. The difference between precipitation and estimated infiltration rate is taken to be the quick storm runoff and is the input to that submodel.

There are two additional parameters, k_i and n_i which must be optimized. The value of l_s can be approximated by an effective hydraulic conductivity, K_{eff} [26]. Bouwer [8] measured K_{eff} to be around half of the corresponding saturated hydraulic conductivity, K. The K values for different soil texture types can be obtained from tables of Rawls et al. [24] or from Singh [26] and V_{i0} is estimated as

$$V_{i0} = f\mathrm{RD}A, \tag{A.5}$$

where RD is the rooting depth. The effective porosity, f, can be obtained from the same sources as K for different soil textures, the FC values (and also porosity) for various soil types and the RD values for different soil type and vegetation combinations are found in Thornthwaite and Mather [30].

When calculating the soil's maximum available storage space, V_0, the concept of the non-active moisture

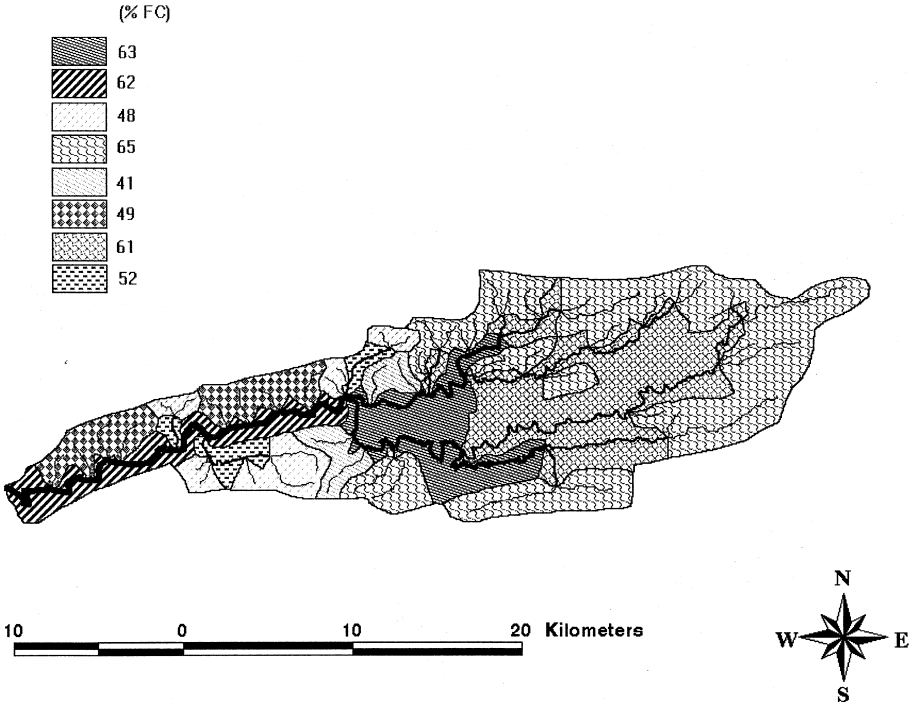

Fig. 11. Simulated sample soil moisture values, in percentage of field capacity (FC), distributed over the subcatchments. 12 PM, 25 November 1992, Mahantango Creek, PA.

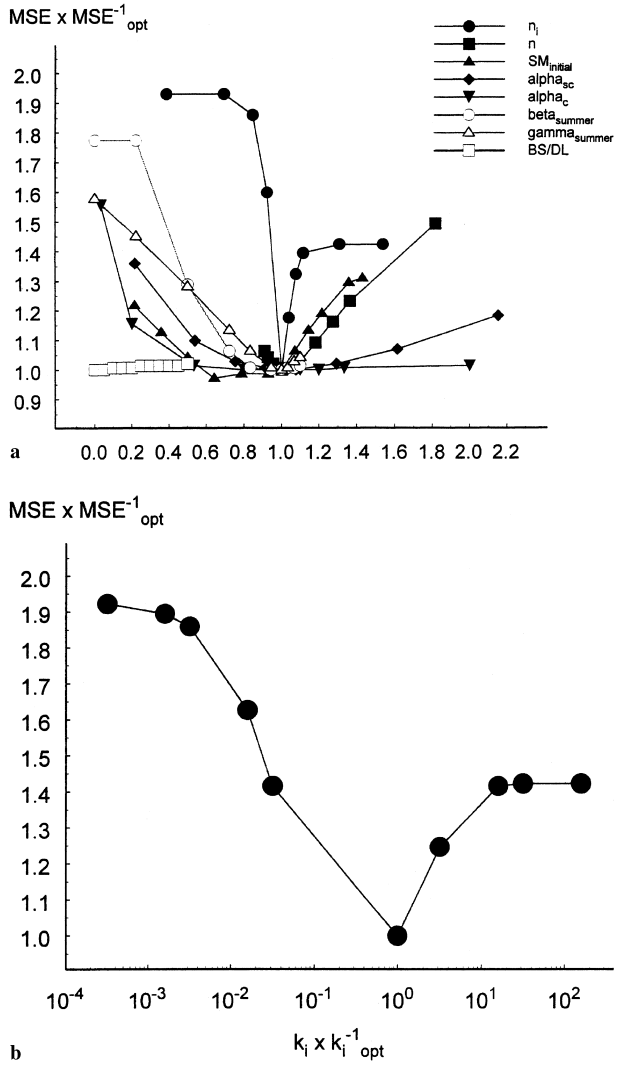

Fig. 12. Sensitivity analysis of the model parameters for the Mahantango Creek, PA watershed. Abscissa: actual parameter value over its optimized value; Ordinate: ratio of the two corresponding mean squared errors between observed and simulated mean daily discharges. Mahantango Creek, PA, calibration period: November 1991–October 1992.

zone used in TOPMODEL [23] is applied. It is assumed in the model that below the root zone, i.e. in the non-active moisture zone, the moisture content of the soil is always close to the field capacity (FC) value [23]. Since the moisture content in this zone is quasi-constant in time, according to our assumption, any water storage dynamics takes place within the root zone. We further assume in the model that any seepage, l_s, from the root zone reaches the unconfined groundwater table without further delay. Capillarity effects and the capillary fringe itself are neglected in the model. In the Holtan model the infiltration rate is driven by the potential storage space which is driven by the accumulated infiltration.

A.3. The evaporation submodel

Evaporation is calculated based on both soil moisture content and potential evaporation, PE [mm day^{-1}], estimates obtained from the Jensen and Haise [17] technique

$$\mathrm{PE} = (1.6742 \cdot 10^{-2})R(0.014(1.8T + 32) - 0.37), \quad \text{(A.6)}$$

where R is incident solar radiation in units of cal cm^{-2} day^{-1}, and T mean monthly air temperature in Celsius. The actual evaporation, E, is estimated [4] as

$$E = \mathrm{PE}\left(1 - \frac{V_i}{V_{i0}}\right). \quad \text{(A.7)}$$

In lieu of measured radiation data an estimate of R can be obtained [21] the following way

$$R = R_e\left(d + e\left(\frac{\mathrm{BS}}{\mathrm{DL}}\right)\right), \quad \text{(A.8)}$$

where R_e is the extraterrestrial radiation in the same units as R, d and e are dimensionless empirical constants, BS the number of hours with bright sunshine and DL the number of daylight hours. In general d and e depend on location, season, and on the state of the atmosphere [9], R_e and DL depend on latitude and time of the year.

Estimated average values of d and e for selected locations as well as R_e values as a function of latitude and time of year can be found in Ref. [9].

A.4. The unconfined groundwater submodel

The groundwater model which describes the unconfined saturated zone dynamics does not increase the number of unknown parameters in the watershed model since all of the new parameters involved can be derived by the application of the Brutsaert and Nieber [10] recession flow analysis [28,29]. For an unconfined aquifer the baseflow recession discharge, Q_{br}, has the following relationship

$$\frac{\mathrm{d}Q_{br}}{\mathrm{d}t} = -aQ_{br}^{b}. \quad \text{(A.9)}$$

Eq. (A.9) plotted as $\log(-\mathrm{d}Q_{br}/\mathrm{d}t)$ versus $\log(Q_{br})$ forms a straight line with a slope of b [–] and intercept a [m$^{3(1-b)}$ s^{b-2}]. The solution of Eq. (A.9) when $b \neq 1$ is

$$Q_{br} = \left(Q_{br0}^{1-b} - (1-b)at\right)^{1/(1-b)}; \quad \text{(A.10)}$$

the solution of Eq. (1) with no inflow is

$$Q = \left(Q_0^{1-n/n} - (1-n)k^{1/n}t\right)^{n/1-n}; \quad \text{(A.11)}$$

and when equating Eq. (A.10) with Eq. (A.11) we obtain

$$n := n_{gw} = \frac{1}{2-b}; \quad k := k_{gw} = \left(\frac{a}{n}\right)^{n}. \quad \text{(A.12)}$$

The recession stream discharge can be linked to the mean groundwater table elevation by inserting k from Eq. (A.12) into Eq. (2) with the help of Eq. (1)

$$h = \frac{Q^{1/n}}{fA\left(\frac{a}{n}\right)}, \tag{A.13}$$

in this way the baseflow rate at any time can be estimated since h is updated through l_s from Eq. (A.2). For the sake of simplicity it is assumed in the model that baseflow contributes only to the main channel of the catchment.

References

[1] ARS-USDA. Miscellaneous Publication No. 1330. Washington, DC: ARS-USDA, 1976.

[2] Baker DG, Haines DA. Solar radiation and sunshine duration relationships in the north-central region and Alaska. Univ Minnesota Ag Exp Station Tech Bull 1969;262:1–372.

[3] Berod DD, Singh VP, Devred D, Musy A. A geomorphologic nonlinear cascade (GNC) model for estimation of floods from small alpine watersheds. J Hydrol 1995;166:147–170.

[4] Beven KJ. Scale considerations. In: Bowles DS, O'Connell PE, editors. Recent advances in the modeling of hydrologic systems. Dordrecht: Kluwer Academic Publishers, 1991:667.

[5] Beven KJ. TOPMODEL: a critique. Hydrological Processes 1997;11:1069–1085.

[6] Beven KJ, Kirkby MJ. A physically-based variable contributing area model of basin hydrology. Hydrological Sci Bull 1979;24:43–69.

[7] Beven KJ, Lamb R, Quinn P, Romanowicz R, Freer J. TOPMODEL. In: Singh VP, editor. Computer models of watershed hydrology. Highlands Ranch, CO: Water Resources Publishers, 1995:1130.

[8] Bouwer H. Rapid field measurement of air entry value and hydraulic conductivity of soil as significant parameters in flow system analysis. Water Resour Res 1966;2:729–738.

[9] Brutsaert W, Evaporation into the atmosphere. Dordrecht: Kluwer Academic Publishers, 1982:299.

[10] Brutsaert W, Nieber JL. Regionalized drought flow hydrographs from a mature glaciated plateau. Water Resour Res 1977;13:637–643.

[11] Dooge JCI. Looking for hydrologic laws. Water Resour Res 1986;22:46s–58s.

[12] Federer CA. Forest transpiration greatly speeds streamflow recession. Water Resour Res 1973;9:1599–1604.

[13] Holtan HN. A concept of infiltration estimates in watershed engineering. USDA Paper 41-51, Washington, DC, 1961.

[14] Horton RE. Rainfall interception. Month Weather Rev 1919;47:603–623.

[15] Horton RE. Erosional development of streams and their drainage basins: hydrophysical approach to quantitative morphology. Bull Geol Soc Am 1945;56:275–370.

[16] Jakeman AJ, Hornberger GM. How much complexity is warranted in a rainfall–runoff model?. Water Resour Res 1993;29:2637–2649.

[17] Jensen M, Haise H. Estimating evapotranspiration from solar radiation. J Irrig Drain, ASCE 1963;89:15–41.

[18] Lighthill J, Whitham GB. Kinematic waves I. Flood movement in long rivers. Proc R Soc London, Ser A 1955;229:281–316.

[19] Nash JE. The form of the instantanous unit hydrograph. Publ IASH 1957;45(3):1114–1121.

[20] O'Connell PE, Todini E. Modelling of rainfall, flow and mass transport in hydrological systems: an overview. J Hydrol 1996;175:3–16.

[21] Prescott JA. Evaporation from a water surface in relation to solar radiation. Trans R Soc South Austral 1940;64:114–125.

[22] Global water cycle: extension across the earth sciences. Progress Report of the Work Plan NASA Earth Observing System NAGW-2686, 1995.

[23] Quinn PF, Beven KJ. Spatial and temporal predictions of soil moisture dynamics, runoff, variable source areas and evapotranspiration for Plynlimon, mid-Wales. Hydrol Process 1993;7:425–448.

[24] Rawls WJ, Brakensiek DL, Miller N. Green-Ampt infiltration parameters from soils data. J Hydra Div ASCE 1983;109:62–70.

[25] Rodriguez-Iturbe I, Valdes JB. The geomorphological structure of hydrologic response. Water Resour Res 1979;15:1409–1420.

[26] Singh VP. Elementary hydrology. Englewood Cliffs, NJ: Prentice-Hall, 1992:973.

[27] Strahler AN. Quantitative analysis of watershed geomorphology. Trans Am Geophys Union 1957;38:913–920.

[28] Szilagyi J, Parlange MB. Baseflow separation based on analytical solutions of the Boussinesq equation. J Hydrol 1998;204:251–260.

[29] Szilagyi J, Parlange MB, Albertson JD. Recession flow analysis for aquifer parameter determination. Water Resour Res 1998;34:1851–1857.

[30] Thornthwaite CW, Mather JR. Introduction and tables for computing potential evapotranspiration and the water balance. Publications in Climatology. Drexel Institute of Technology, 1957:X(3).

[31] Trimble GR. A problem analysis and program for watershed management research, Northeast forest experiment station. Station Paper 116. Washington, DC: US Forest Service, 1959.

[32] Official Soil Series Descriptions. Unites States Department of Agriculture. Natural Resources Conservation Service, Soil Survey Division, Web site, 1997.

[33] Viessman Jr W, Lewis GL, Knapp JW. Introduction to hydrology. New York: Harper & Row, 1989:780.

[34] Zecharias YB, Brutsaert W. The influence of basin morphology on groundwater outflow. Water Resour Res 1988;24:1645–1650.